Epitaxial $Bi_3Fe_5O_{12}$(001) films grown by pulsed laser deposition and reactive ion beam sputtering techniques

N. Adachi, V. P. Denysenkov, S. I. Khartsev, and A. M. Grishin[a)]
Department of Condensed Matter Physics, Royal Institute of Technology, S-100 44 Stockholm, Sweden

T. Okuda
Nagoya Institute of Technology, Nagoya 466, Japan

(Received 17 December 1999; accepted for publication 24 May 2000)

We report on processing and comparative characterization of epitaxial $Bi_3Fe_5O_{12}$ (BIG) films grown onto $Gd_3(ScGa)_5O_{12}$[GSGG,(001)] single crystal using pulsed laser deposition (PLD) and reactive ion beam sputtering (RIBS) techniques. A very high deposition rate of about 0.8 μm/h has been achieved in the PLD process. Comprehensive x-ray diffraction analyses reveal epitaxial quality both of the films: they are single phase, exclusively (001) oriented, the full width at half maximum of the rocking curve of (004) Bragg reflection is 0.06 deg for PLD and 0.05 deg for RIBS film, strongly in-plane textured with cube-on-cube film-to-substrate epitaxial relationship. Saturation magnetization $4\pi M_s$ and Faraday rotation at 635 nm were found to be 1400 Gs and -7.8 deg/μm in PLD-BIG, and 1200 Gs and -6.9 deg/μm in RIBS-BIG. Ferromagnetic resonance (FMR) measurements performed at 9.25 GHz yielded the gyromagnetic ratio $\gamma = 1.797\times 10^7$ l/s Oe, 1.826×10^7 l/s Oe; the constants of uniaxial magnetic anisotropy were $K_u^* = -8.66\times 10^4$ erg/cm^3, -8.60×10^4 erg/cm^3; the cubic magnetic anisotropy $K_1 = -2.7\times 10^3$ erg/cm^3, -3.8×10^3 erg/cm^3; and the FMR linewidth $\Delta H = 25$ and 34 Oe for PLD and RIBS films correspondingly. High Faraday rotation, low microwave loss, and low coercive field $\leqslant$40 Oe of BIG/GSGG(001) films promise their use in integrated magneto-optic applications. © *2000 American Institute of Physics.* [S0021-8979(00)03317-X]

I. INTRODUCTION

Completely substituted bismuth iron garnet $Bi_3Fe_5O_{12}$ (BIG) films have attracted much attention for various applications in nonreciprocal and waveguide devices, based on magnetostatic waves (MSW), magneto-optical (MO) isolators, and integrated MSW-MO components. Since Bi substituted yttrium iron garnet (YIG) possesses enhanced Faraday effect of -2 deg/μm at 633 nm per Bi content and low optical losses in the visible to near infrared light region, there were many attempts undertaken to increase Bi substitution in Bi:YIG films made by liquid phase epitaxy. Furthermore, it has been found that linear dependence of Faraday rotation on Bi content changes to a superlinear one when the Bi content exceeds two atoms per one formula unit and reaches the giant value as high as -8 deg/μm for completely substituted BIG.

Bi^{3+}, having been substituted in dodecahedral sites of garnet structure, has a large ionic radius of 1.17 Å compared to 0.95 Å of Y^{3+}. This results in very strong YIG lattice expansion with the rate of 0.083 Å/(Bi atom/formula unit). At high temperatures combinatorial entropy becomes energetically favorable and makes $Bi_3Fe_5O_{12}$ to be a thermodynamically nonequilibrium phase. This is why completely substituted BIG has been obtained only in the form of a film clamped on the single crystal substrate. A first time BIG(111) film has been grown by a reactive ion beam sputtering (RIBS) technique onto $Gd_3(ScGa)_5O_{12}$ (GSGG) substrate[1] and exhibited -8.4 deg/μm of Faraday rotation at 633 nm and saturation magnetization $4\pi M_s = 1500$ Gs.[2] In the last decade BIG films had also been prepared by electron cyclotron resonance (ECR) sputtering and radio-frequency (rf) magnetron sputtering techniques.[3,4] These methods show approximately equal results, however, all of them suffer from too low deposition rate to provide industrial BIG application.

Pulsed laser deposition (PLD) thin film technology has made rapid progress in recent years.[5] Great success has been achieved to grow high-T_c superconducting thin films, ferroelectrics, manganite colossal magnetoresistors, high performance dielectrics, and complex oxide multilayers.[6] In comparison with other techniques, PLD has great advantages using laser radiation as a source of ''pure'' energy: film contamination can be suppressed to the lowest level while PLD is capable of operating at relatively high gas pressure that might be critical for complex oxide film growth.

Two attempts to prepare BIG by PLD have been recently reported.[7,8] Films of (111) BIG grown by Chern and Liaw[7] exhibit Faraday rotation of -5.4 deg/μm at 633 nm and $4\pi M_s = 1470$ Gs. Watanabe *et al.* fabricated (111) BIG with Faraday rotation of -7.0 deg/μm at 633 nm.[8] In this article we report on preparation and comprehensive characterization of BIG films made by PLD and RIBS techniques to compare films crystalline and magneto-optical properties, magnetic performance at low and high frequencies.

[a)]Electronic mail: grishin@kth.se

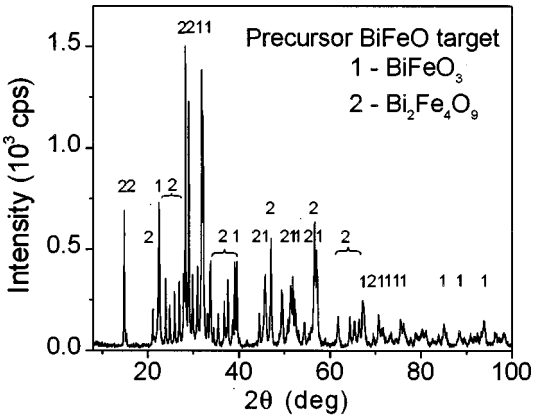

FIG. 1. X-ray diffraction (XRD, Cu$K\alpha$ radiation) pattern of the target used for pulsed laser deposition. The peaks denoted ''1'' and ''2'' correspond to Bragg reflections from $BiFeO_3$ (JCPDS 14-181) and $Bi_2Fe_4O_9$ (JCPDS 25-090) oxides, respectively.

II. FILMS SYNTHESIS

In the reactive ion beam sputtering (RIBS) technique, Kaufman type ion (usually Ar^+) source is used to produce uniform ion beam to sputter the target. Argon ions are neutralized to prevent charge accumulation on the insulating target. A reactive atmosphere for growing film oxidation is formed by supplying O_2 gas in the vicinity of substrate holder. The detailed description of BIG preparation by RIBS technique can be found in Ref. 9. Usually it takes about 10 h to get micrometer thick BIG film.

In the PLD process, KrF excimer laser (LPX300, Lambda Physik, $\lambda = 248$ nm, pulsed energy density 2–3 J/cm^2, the repetition rate 30–50 Hz) has been used to ablate ceramic target. Both RIBS and PLD techniques use precursor target, which was made from oxide powders $3 \times Bi_2O_3 + 5 \times Fe_2O_3$ by cold pressing at 300 kg/cm^2 and sintering at the temperature 800–900 °C for 4 h. The procedure of regrinding, pressing, and sintering was repeated twice to ensure microscopic homogeneity. The density of the target is 6.09 g/cm^3. X-ray diffraction (XRD) analysis confirms the target to be two phases: $BiFeO_3$ and $Bi_2Fe_4O_9$ (Fig. 1) with the stoichiometric Bi:Fe ratio of 3:5, which is requested for $Bi_3Fe_5O_{12}$ garnet phase. During a deposition the target was rotated to avoid its fast erosion and consumption.

(001) $Gd_3(ScGa)_5O_{12}$ garnet (GSGG) single crystal has been chosen as a substrate. It has a cubic lattice constant of 12.570 ± 0.005 Å. Thus the mismatch between GSGG and fabricated BIG film appeared to be less than 0.5%. GSGG wafer has been sliced into square 5×5 mm^2 pieces and bonded to the heater by a silver paste. The substrate was heated at 650 °C before deposition for thermal cleaning of the surface, and then during the deposition the substrate was kept at growth temperature of 550 °C. The distance between the substrate and the target was set at 5 cm and typical deposition time was about one hour. The oxygen pressure has been varied from 5 to 200 mTorr. The processing conditions used in PLD and RIBS techniques are summarized in Table I.

TABLE I. Processing conditions for PLD and RIBS techniques.

	PLD	RIBS
Target	Precursor $BiFeO_3$ and $Bi_2Fe_4O_9$ ceramics	
Background pressure, Torr	1×10^{-7}	2×10^{-6}
Working pressure, mTorr	5–200	0.11
Substrate	$Gd_3(ScGa)_5O_{12}(001)$, $a = 12.570 \pm 0.005$ Å	
Film lattice constant, Å	12.627	12.633
Substrate temperature, °C	550	480
Deposition rate, μm/h	0.730	0.128

III. FILMS CHARACTERIZATION

Both PLD and RIBS films were characterized by the same methods using the same equipment. Film thickness was measured by the atomic force microscope (AFM, Burleigh Personal SPM). To make a sharp step of the film a small part of the substrate was masked before the deposition or a small part of the film was etched away by the acid. Thickness of the films deposited by PLD and RIBS during one hour was estimated to be 0.730 and 0.128 μm correspondingly, thus the deposition rate achieved by PLD technique is six times higher than that in RIBS technique. Both films have red color and optically smooth surface. The optical absorption coefficient α at 635 nm was measured to be 3484 cm^{-1} for both films.

A *Siemens D-5000* powder x-ray diffractometer with Cu tube has been used to study the films' crystalline structure. XRD patterns of PLD films grown at oxygen pressure exceeding 30 mTorr show weak (012) $BiFeO_3$ Bragg peak while films grown at lower oxygen pressure have been found to be single $Bi_3Fe_5O_{12}$ phase. Instead of a complicated two phase XRD pattern of the target (Fig. 1), an XRD θ–2θ scan of PLD-BIG/GSGG structure (Fig. 2) consists of (00l) Bragg reflections only. Cu $K_{\alpha 1}$ and Cu $K_{\alpha 2}$ lines from BIG film and GSGG substrate are clearly resolved. At low incident θ angles the intensity of the film reflections are higher compared with those from the substrate due to smaller x-ray penetration depth. In logarithmic scale, besides the main (004), (008), (0012), and (0016) reflections, the weaker

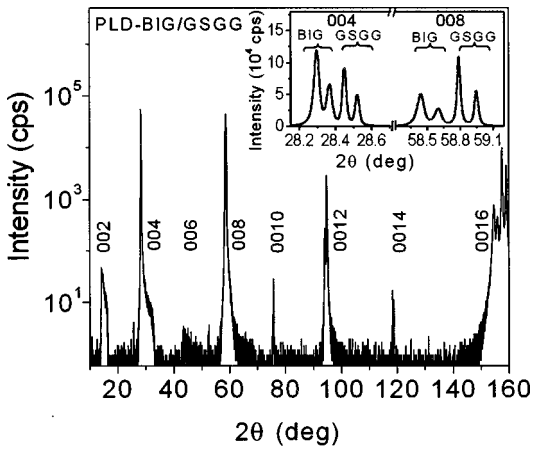

FIG. 2. XRD θ–2θ scans in Cu$K\alpha$ radiation for 0.73-μm-thick $Bi_3Fe_5O_{12}$(BIG) film grown by PLD technique onto $Gd_3(ScGa)_5O_{12}$(GSGG) single crystal. (*hkl*) peaks indicate BIG film and GSGG substrate Bragg reflections. Magnified (004) and (008) reflections are shown in the insert.

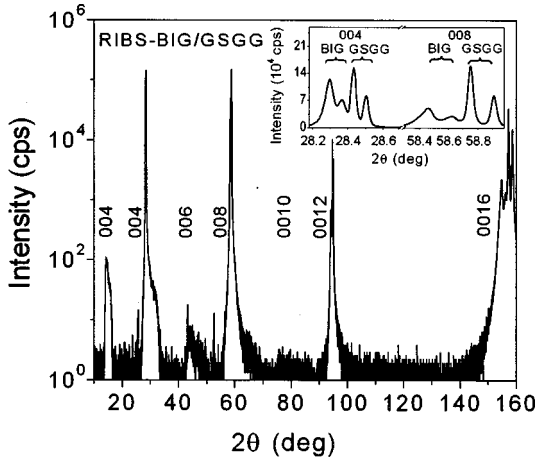

FIG. 3. Same XRD patterns as in Fig. 2 for RIBS-made $Bi_3Fe_5O_{12}$ (1.28μm)/$Gd_3(ScGa)_5O_{12}$ structure.

peaks can be recognized around $2\theta = 14°$, 43°, 75°, and 120°. They correspond to (002), (006), (0010), and (0014) reflections, which are forbidden in ideal crystal and attributed to the noncomplete destructive interference of x rays on GSGG surface distorted by cutting and polishing processes. Figure 3 shows similar θ–2θ XRD patterns for BIG film grown onto GSGG substrate by RIBS technique.

Films' lattice parameter a_0 has been found by plotting a_0 against the Nelson–Riley function[10]

$$\frac{a_{\cos\theta} - a_0}{a_0} = C\cos^2\theta\left(\frac{1}{\sin\theta} + \frac{1}{\theta}\right), \tag{1}$$

where $a_{\cos\theta}$ is an interplane distance calculated from the apparent Bragg peak position at 2θ and C is a fitting coefficient. Figure 4 presents the lattice parameters $a_{\cos\theta}$ calculated from (004), (008), (0012), and (0016) Bragg reflections for PLD, RIBS films as well as for GSGG substrate. The ''true'' lattice parameters a_0, obtained as an extrapolation to $\cos^2\theta \to 0$, were found to be 12.574 Å for GSGG substrate,

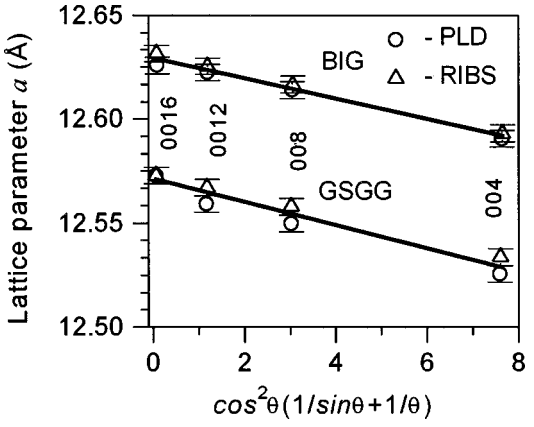

FIG. 4. Lattice parameters for $Gd_3(ScGa)_5O_{12}$ substrate and $Bi_3Fe_5O_{12}$ films grown by PLD (symbols ○) and RIBS (symbols △) techniques. Lattice parameter $a_{\cos\theta}$ was calculated from (004), (008), (0012), and (0016) Bragg reflections position. Experimental $a_{\cos\theta}$ vs θ dependence has been fitted to Nelson–Riley Eq. (1) to extrapolate at $\cos\theta \to 0$ ''true'' lattice parameters $a_0 = 12.574$ Å for GSGG substrate, 12.627 Å for PLD-BIG, and 12.633Å for RIBS-BIG film.

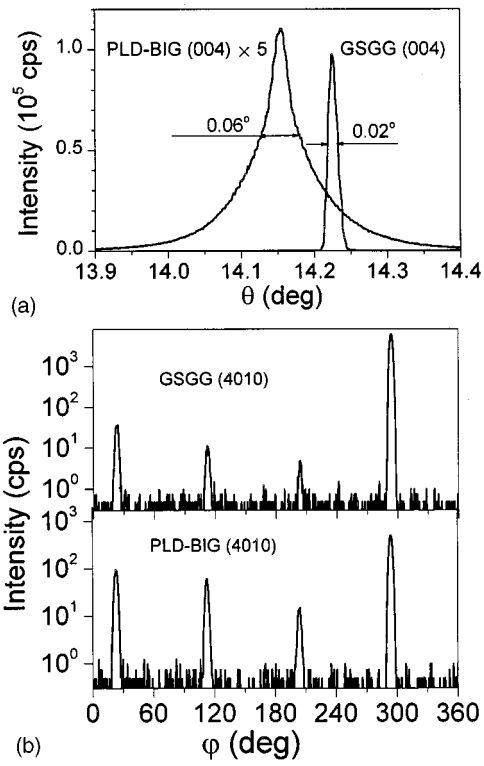

FIG. 5. XRD patterns for 0.73-μm-thick PLD-BIG(001) film: (a) rocking curves of (004) Bragg reflections from $Bi_3Fe_5O_{12}$(BIG) film and $Gd_3(ScGa)_5O_{12}$(GSGG) substrate; (b) φ scans of off-normal (4010) plane in BIG film and GSGG substrate.

12.627 Å for PLD-BIG film, and 12.633 Å for RIBS-BIG. Taking into account the Bragg reflections linewidth, shown in Fig. 4 as error bars, the lattice parameters of both PLD and RIBS films can be regarded to be the same within the experimental errors while the lattice mismatch between the BIG films and GSGG substrate is estimated to be less than 0.5%.

The rocking curves of (004) reflections of PLD and RIBS films in comparison with GSGG substrate are shown in Figs. 5 and 6. The full width at half maximum (FWHM) is 0.06° for the PLD film and 0.05° for the RIBS film, respectively. The narrowest FWHM of PLD-BIG has been achieved for the film grown at oxygen pressure of 10 mTorr. We also detected Bragg reflections from off-normal {4010} planes of GSGG and BIG. They are presented as φ scans in Figs. 5 and 6. The optimum sample θ_{sample} and the detector $2\theta_{\text{detector}}$ positions used for φ-scan measurements are shown in Table II. Fourfold symmetry observed in φ scans and strict correspondence between diffraction peaks from film and substrate confirm epitaxial cube-on-cube relationship of $Bi_3Fe_5O_{12}$ on $Gd_3(ScGa)_5O_{12}$

$$(001)\text{BIG}\|(001)\text{GSGG},$$

$$[010],[100]\text{BIG}\|[010],[100]\text{GSGG}.$$

High crystalline performance of fabricated BIG films results also in narrow linewidth of the ferromagnetic resonance (FMR). FMR measurements were performed at room temperature by the broad-band spectrometer using the *HP*8722*D* Network Analyzer simultaneously as a source and a receiver of microwave signal. Figure 7 shows the typi-

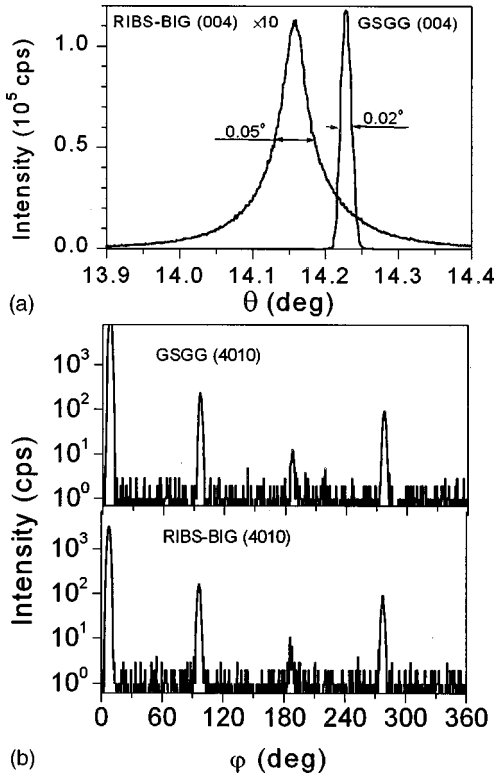

FIG. 6. Same XRD patterns as in Fig. 5 for $Bi_3Fe_5O_{12}(0.128\,\mu m)/Gd_3(ScGa)_5O_{12}$ structure fabricated by RIBS technique.

cal records of FMR differential absorption at 9.25 GHz in PLD and RIBS films in magnetic field perpendicular to the film surface. The FMR linewidth at 9.25 GHz at room temperature in PLD and RIBS films in magnetic field perpendicular to the film surface was found to be $\Delta H = 25$ and 34 Oe for PLD and RIBS film, respectively. The linewidth of PLD-BIG is the narrowest in comparison with the results for PLD-made BIG(111) reported earlier.[7,8] The occurrence of FMR in PLD-BIG in magnetic field is weaker than that in RIBS. One displays lower magnetic anisotropy in PLD film compared with RIBS-BIG. To quantify magnetic anisotropy, the angular dependence of the resonance field has been measured (see Fig. 8). The resonance field reaches the minimum value in magnetic field parallel to the film plane, indicating in-plane magnetic anisotropy in PLD- and RIBS-made BIG(001) films. We have used the computational method, similar to that proposed by Makino and Hidaka,[11] to fit experimental polar angle dependence of the resonance field in Fig. 8 by theoretical curve. Three fitting parameters, giving the best fit to experimental data, were as follows the gyromagnetic ratio $\gamma = 1.797\times10^7$ and 1.826×10^7 l/s Oe; the effective constant of uniaxial anisotropy $K_u^* = -8.66\times10^4$ and -8.60×10^4 erg/cm^3; and the constant of cubic magnetic anisotropy $K_1 = -2.7\times10^3$ and -3.8×10^3 erg/cm^3 for PLD and RIBS film correspondingly.

TABLE II. Sample and detector positions used for (4010) φ scans presented in Figs. 5 and 6.

(4010) Bragg reflection	PLD		RIBS	
	θ_{sample} (deg)	$2\theta_{detector}$ (deg)	θ_{sample} (deg)	$2\theta_{detector}$ (deg)
GSGG	63.174	82.599	63.231	82.525
BIG	62.830	82.099	63.078	82.161

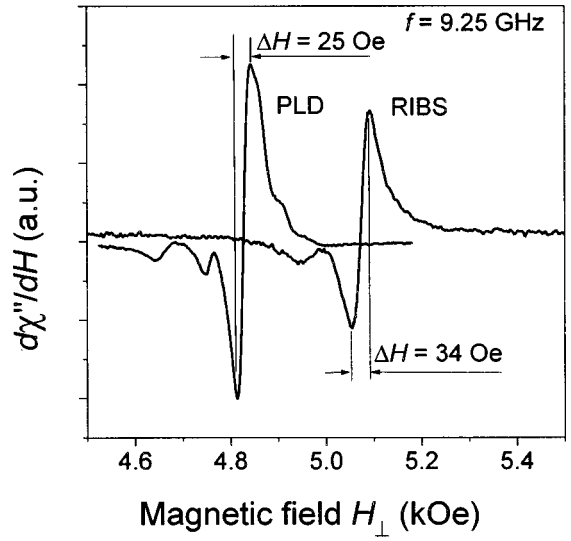

FIG. 7. Ferromagnetic resonance (FMR) absorption in PLD- and RIBS-made BIG(001) films measured at 9.25 GHz in magnetic field perpendicular to the film.

The magnetization $M(H)$ in fabricated BIG films was measured by vibrating sample magnetometer [(VSM) *Oxford Instruments*] whereas the Faraday rotation $\theta_F(H)$ at 635 nm was recorded in pulsed magnetic field (raising time 2.7 ms, maximum magnetic field 20 kOe). Figures 9 and 10 show $M(H_\parallel)$ and $M(H_\perp)$ magnetization loops in parallel and perpendicular magnetic field, as well as Faraday rotation $\theta_F(H_\perp)$ hysteresis loops for PLD and RIBS BIG films. Para-

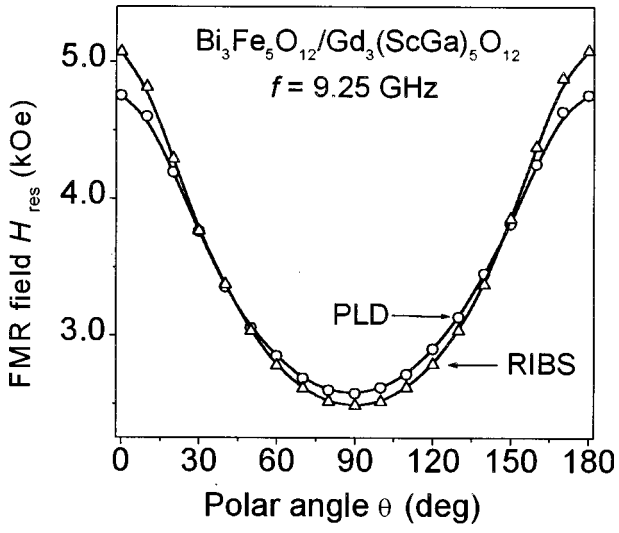

FIG. 8. Angular dependence of the ferromagnetic resonance (FMR) field measured at 9.25 GHz. The polar angle θ is the angle between the external magnetic field, rotating in the (010) plane, and the normal to the film surface. The experimental data for PLD (symbols ○) and RIBS (symbols △) BIG(001) films have been fitted to the theoretical curves, shown by solid lines, by variation of three fitting parameters: gyromagnetic ratio γ, effective constant of uniaxial anisotropy K_u^*, and the constant of cubic anisotropy K_1, presented in Table III.

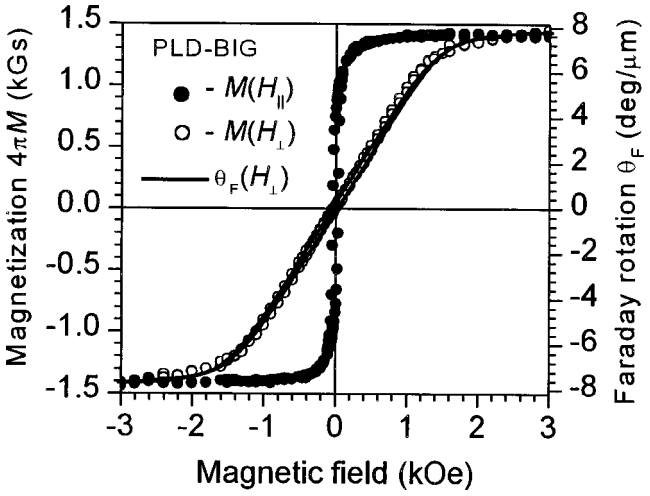

FIG. 9. Pulsed laser deposited 0.73-μm-thick $Bi_3Fe_5O_{12}$ film. Magnetization M vs H in magnetic field parallel $\mathbf{H}_{\|}$ (symbols ●) and perpendicular $\mathbf{H}_{\perp}$ (symbols ○) to the film measured by vibrating sample magnetometer. Solid line shows Faraday rotation θ_F vs $H_{\perp}$ at 635 nm. Paramagnetic contribution from $Gd_3(ScGa)_5O_{12}$ substrate has been subtracted.

magnetic contribution from GSGG substrate has been subtracted. The saturation magnetization $4\pi M_s$ has been estimated to be about 1400 Gs for PLD film and 1200 Gs for RIBS film.

In $\mathbf{H}_{\|}$ geometry, magnetization saturates at rather low magnetic field ($\leqslant$600 Oe). In perpendicular magnetic field $\mathbf{H}_{\perp}$, M-$H_{\perp}$ curves saturate at higher fields $\geqslant$1.6 kOe. We have used the expression for the saturation magnetic field in ''hard'' direction

$$H_{\text{sat}}=\frac{2|K_u^*|}{M_s} \tag{2}$$

as an alternative to FMR tool to determine the effective constant of uniaxial anisotropy K_u^*. Substituting the experimental H_{sat} data to Eq. (2) we obtain $|K_u^*|=8.5\times10^4$ erg/cm^3 for PLD film and 8.2×10^4 erg/cm^3 for RIBS film. With the experimental accuracy, higher for FMR and much lower for VSM measurements, the measured K_u^* constants coincide with each other. Coercive force did not exceed 40 Oe for both of the films. The saturated Faraday rotation of PLD film shows -7.8 deg/μm and that of RIBS film is -6.9 deg/μm. Taking into account the errors in the estimation of thickness and volume of the films, it is suggested that both films show almost the same magnetic and magneto-optical properties. These results, presented in Table III, support the conclusion that BIG films of high crystalline quality have been grown by PLD technique.

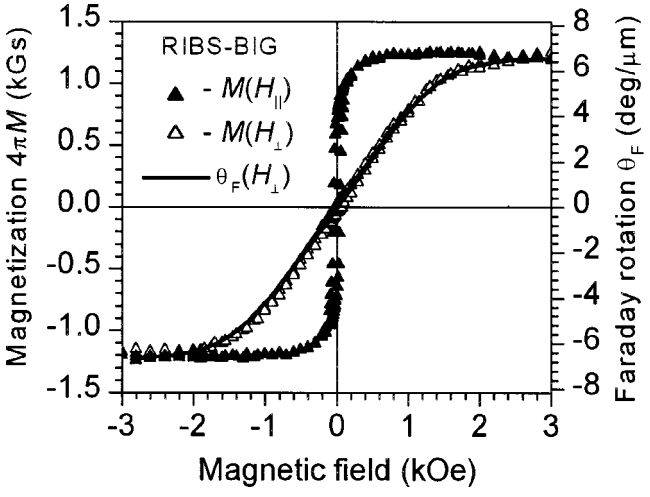

FIG. 10. Same $M-H$ and θ_F-H hysteresis loops as in Fig. 8 for $Bi_3Fe_5O_{12}$(0.128 μm)/$Gd_3(ScGa)_5O_{12}$ structure fabricated by RIBS technique.

TABLE III. Magnetic characteristics of $Bi_3Fe_5O_{12}$ films fabricated by PLD and RIBS techniques.

	PLD	RIBS
Magnetization $4\pi M_s$, Gs	1400	1200
Faraday rotation θ_F, deg/μm	−7.8	−6.9
Gyromagnetic ratio γ, $\times10^7$ 1/s·Oe	1.797	1.826
Effective constant of uniaxial anisotropy K_u^*, $\times10^4$ erg/cm^3	−8.66	−8.60
The constant of cubic anisotropy K_1, $\times10^3$erg/cm^3	−2.7	−3.8
FMR linewidth @9.25 GHz and 300 K, Oe	25	34

Recently we found the Faraday rotation of Ce-substituted YIG films made by PLD is remarkably dependent on the oxygen pressure: θ_F experienced change 2.2 times when oxygen pressure has been varied from 10 to 100 mTorr.[12] A similar effect was observed for PLD-BIG: film performance is highly sensitivity to oxygen pressure in the range 5–200 mTorr. PLD-BIG(001) with superior crystalline and magneto-optical performance has been prepared at 10 mTorr of O_2.

In comparison with the results reported on RIBS-BIG(111),[1,2] the absolute values of saturation magnetization and Faraday rotation obtained in this study for RIBS-BIG(001) film were found to be smaller. At present, the exact origin of the difference in properties of (111) and (001) BIG films as well as the difference in $4\pi M_s$ of PLD-made and RIBS films are obscure, however, we have evaluated the performance of both PLD and RIBS films grown onto the same substrate, with the same size, using the same instruments. This is the most reliable way to make comparative quality test and confirm PLD-BIG shows the performance approaching the RIBS.

IV. CONCLUSIONS

Completely substituted bismuth iron garnet $Bi_3Fe_5O_{12}$(001) films have been successfully grown by KrF pulsed laser deposition and reactive ion beam sputtering techniques and film performance has been compared with each other. PLD yields six times higher deposition rate than that of RIBS technique, which is of great advantage for industry application. The epitaxial quality of BIG films grown onto $Gd_3(ScGa)_5O_{12}$ substrate has been proven by comprehensive x-ray analyses. In-plane magnetization, low coercive field $\leqslant$40 Oe, low microwave loss (FMR linewidth ΔH = 25 Oe@9.25 GHz), and high Faraday rotation of -7.8 deg/μm @635 nm make BIG/GSGG(001) thin film structures attractive for integrated magneto-optic applications.

ACKNOWLEDGMENTS

The authors would like to thank Jesper Wittborn for his help in thickness measurements by AFM and Huonju Kim for useful discussions. This work was supported by the Swedish Natural Sciences Research Council (NFR) and Ministry of Education, Science, Sports, and Culture of Japan (Monbusho).

[1] T. Okuda, N. Koshizuka, K. Hayashi, K. Satoh, H. Taniguchi, and H. Yamamoto, IEEE Trans. J. Magn. Jpn. **3**, 483 (1988).
[2] T. Okuda, T. Katayama, H. Kobayashi, and N. Kobayashi, J. Appl. Phys. **67**, 4944 (1990).
[3] A. Thavendrarajah, M. Pardavi-Horvath, P. E. Wigen, and M. Gomi, IEEE Trans. Magn. **25**, 4015 (1989).
[4] S. Mino, M. Matsuoka, A. Tate, A. Shibukawa, and K. Ono, Jpn. J. Appl. Phys., Part 1 **31**, 1786 (1992).
[5] *Pulsed Laser Deposition of Thin Films*, edited by D. B. Chrisey and G. K. Hubler (Wiley, New York, 1994), pp. 10–19.
[6] D. Dijkkamp, T. Venkatesan, X. D. Wu, S. A. Shaheen, N. Jisrawi, Y. H. MinLee, W. L. McLean, and M. Croft, Appl. Phys. Lett. **51**, 619 (1987).
[7] M. Y. Chern and J. S. Liaw, Jpn. J. Appl. Phys., Part 1 **36**, 1049 (1997).
[8] N. Watanabe, N. Takahashi, and K. Tsushima, Mater. Chem. Phys. **54**, 173 (1998).
[9] T. Okuda, N. Koshizuka, K. Hayashi, T. Takahashi, H. Kotani, and H. Yamamoto, IEEE Trans. J. Magn. **MAG-23**, 3491 (1988); Proc. Int. Sympo. Magneto-Optics, J. Magn. Soc. Jpn. **11**, Suppl. S1 179 (1988).
[10] B. D. Cullity, *Elements of X-Ray Diffraction* (Addison-Wesley, Reading, MA, 1988).
[11] H. Makino and Y. Hidaka, Mater. Res. Bull. **16**, 957 (1981).
[12] H. Kim, A. M. Grishin, K. V. Rao, S. C. Yu, R. Sbiaa, and H. Le Gall, IEEE Trans. Magn. **35**, 3163 (1999).